Characterization of Conducting Poly(3-methylthiophene) Films Prepared Under Sono-Electrochemical Conditions

A. Galal

Department of Chemistry, College of Science, University of Cairo, 12613 Giza, Egypt

Received 29 October 2005; accepted 21 January 2006
DOI 10.1002/app.24513
Published online in Wiley InterScience (www.interscience.wiley.com).

ABSTRACT: Poly(3-methlthiophene) films were prepared under ''silent'' and ''sono-electrochemical'' potentiostatic (SEP) conditions. A three-electrode one-compartment sono-cell was used with a working platinum disc electrode. The sono-electrochemically formed polymer films were deposited with different working electrode-to-horn distances. The composition, electrochemical, spectroscopic, and morphological characteristics of the resulting polymer films were determined. Elemental analysis, FTIR-spectra, and X-ray photoelectron spectroscopy (XPS) data proved that the polymer films prepared under SEP conditions have predominant α-α′-couplings between the 3MT units, and the aromatic ring integrity is maintained in the film. Scanning electron microscopy showed that those films are more compact and less porous compared to the films prepared under silent conditions. The use of sono-irradiation during electropolymerization enhanced the diffusion of the monomer units towards the electrode surface and resulted in relatively less doped polymers with less conductivity. Electrochemical impedance spectroscopy (EIS) data for films prepared under silent and SEP conditions were collected in a monomer-free solution. The results show that the impedance of SEP films is relatively higher than those prepared under silent conditions, and a combination of charge transfer kinetics with diffusion-controlled conduction mechanism within the films. The diffusion was found to be a function of the porosity of the film. Conductivity measurements are in good agreement with EIS, elemental analysis, and XPS data. © 2006 Wiley Periodicals, Inc. J Appl Polym Sci 102: 2416–2425, 2006

Key words: electropolymerization; poly(3-methylthiophene); sono-electrochemistry; EIS; SEM; XPS

INTRODUCTION

Conducting polymers continues to attract the attention and interest of researchers for their possible applications as sensors,[1] for the design of conducting paints,[2] opto-electronic applications,[3] surface protection against corrosion,[4] and as composite with gold for the formation of nanomaterials.[5,6] Electrochemical methods were used extensively for the preparation of this class of materials and the properties of the resulting films were also studied. On the other hand, other methods have been used to synthesize conducting polymer films for specific applications. Thus, large size anisotropic poly (pyrrole) with actuation properties have been prepared on poly(tetra-fluoroethylene) walls.[7] The resulting polymer film could be used as an artificial muscle. Also, thin films of conducting polymeric materials were deposited on several substrates using an inductively coupled pulsed-plasma reactor.[8] The morphology and electrical properties of the resulting films were dependent on the positioning of the substrate inside the RF reactor.

A unique method depending on sono-energy was recently employed to obtain conducting polymeric films. Barton et al.[9] showed that highly sensitive and inexpensive microelectrode arrays for biosensors applications could be fabricated sono-chemically. Sonogashira coupling was used as a method to obtain phenylene type conjugated polymers.[10] Moreover, the preparation of nanocomposites embedded conducting polymers was possible using sono-chemical methods.[11] The electrochemical characterization using voltammetry for colloidal solution and modified electrodes made of cast-films of poly(aniline) prepared under ultrasonic irradiation showed that the films are highly electroactive.[12] Several excellent articles showed the effect of sono-power on electrochemical oxidation of organic compounds,[13] voltammetric analysis,[14] and electrode surface modification.[15] Thiophene films were grown under ultrasonic field and the mechanical properties as well as the resulting polymer conductivity were affected by the presence and absence of irradiation field.[16] It was also reported that the rate of electro-initiated cationic copolymerization of isoprene and α-methylstyrene depended on the sono-irradiation, polymerization potential, copolymer composition, and their corresponding reactivity ratio.[17] However, further information on the electronic, spectral, and morphological properties of poly(3-methylthiophene), an important class of conducting polymers, prepared under sono-electrochemical conditions has not been cited in the literature.

Correspondence to: A. Galal (galalah@chem-sci.cu.edu.eg).

Polymer films prepared under sono-electrochemical conditions have different morphological structures that should result in different electrochemical and electronic characteristics. The aim of this work is to prepare poly(3-methylthiophene) systematically under different sono-electrochemical conditions, mainly with different irradiation power and electrode-to-irradiation source distance. The polymer films prepared under these conditions should possess different electrochemical/electrical and morphological characteristics than that prepared under silent conditions. Thus, the electrochemical properties are studied using cyclic voltammetric and AC impedance techniques, the spectral characteristics of as-grown thin films are measured, and their morphology are also determined. The electrical conductivity of the films were measured using the four-probe method and were related to the voltammetry and electrochemical impedance spectroscopy (EIS) data.

EXPERIMENTAL

Polymer films were deposited on a BAS (West Lafayette) MF-2013 platinum disc electrode or on a 6 mm radius platinum rod (embedded in a Teflon jacket) electrode (Alfa Aesar, WI). A platinum sheet ($2.0 \times 3.0\ cm^2$) was used as a counter electrode and all potentials were referred to a saturated Ag/AgCl electrode. 3-Methylthiophene (3MT), tetra-butyl ammonium tetra-fluoroborate (TBATFB), lithium perchlorate (LPC), and acetonitrile (AcN) were high purity grade reagents from Aldrich Chem. (Milwaukee, USA) and were used as received without further purification. Polymer synthesis was carried out in a three-electrode one-compartment glass cell. The cell configuration allowed the insertion of the working electrode from the bottom and the tip of the horn that was attached to the power supply of the sonication device was inserted from the top as indicated in the schematic diagram of Figure 1. A length scaling in centimeter graduation, with 0.1 cm precision, was placed on the outer wall of the cell to control the distance separation between the working electrode and the tip of the horn. Nitrogen gas was introduced into the electrolyte containing the monomer prior to the start of the polymerization, and was kept as a blanket over the solution surface throughout the experimental measurements. The working electrode was polished using soft cloths and alumina paste slurry ($< 0.2\ \mu m$), rinsed with distilled water, thoroughly washed with AcN, and dried.

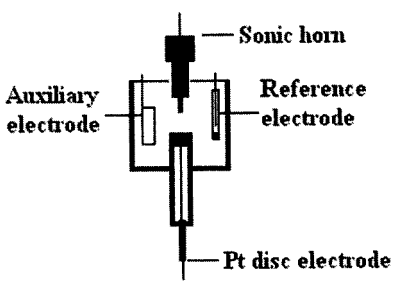

Figure 1 Schematic diagram of the one-compartment three-electrode cell used for the sono-electrochemical preparation of polymer films.

A BAS-100B electrochemical analyzer was used for the electrochemical deposition of the poly(3-methylthiophene) (PMT) films using a constant applied potential of +1.75 V in presence (sono-electrochemical deposition) and absence (silent electrochemical deposition) of the sono-irradiation power. A Gamry PC3/750 potentiostat/galvanostat/ZRA system (Wilmington, USA) was used for EIS and cyclic voltammetry (CV) measurements. This system was interfaced to a personal computer to control the experiments and the data were analyzed using Gamry CMS-300 framework/analysis software. A VC130 (Betatek, Ontario, Canada), 20-kHz ultrasonic horn transducer systems with a stepped 3 mm micro tip titanium alloy were employed. For intensity of 20%, the corresponding power is 210 W cm^{-2}. The horn probe was applied in a face-on geometry to the working electrode and positioned at a constant distance of 30–50 mm. For polymer films prepared for SEM and FTIR experiments, a platinum sheet ($2 \times 2cm^2$) connected to a platinum wire replaces the disc-working electrode. The electrical conductivities of the films synthesized were measured using a four-point probe for conducting polymer electrode studies.[18] FTIR experiments were performed using a Nicolet Impact 400 FTIR instrument (Nicolet, USA). Electron spectroscopy for chemical analysis (ESCA) was performed using the Perkin-Elmer ESCA-5300 Spectrometer with pass energy of about 25 eV ($\Delta E = 0.5$ eV). A Cambridge Stereoscan 600 instrument (Boston, USA) with typically 5/25 kV was used to obtain the scanning electron micrographs (SEM).

The silent electrochemical and sono-electrochemical deposition of the conducting polymer films was carried out from a solution consisting of 0.1*M* TBATFB or LPC, 0.05*M* monomer dissolved in dry AcN. CV experiments conditions are as indicated in the results section for the potential limits and scan rate used. The CV and EIS measurements on the polymer film were carried out at room temperature ($20^\circ C \pm 2^\circ C$) in a monomer-free solution containing 0.1*M* TBATFB/AcN. The exposed sample area was 0.282 cm^2. The data analysis software applied nonlinear least squares fitting with Levenberg-Marquardt/Simplex algorithms.[19] Prior to performing the impedance measurements, the polymer film was subjected to a constant potential of −0.2 V for 10 min to ensure undopping of anions that was achieved when a stable current readings were measured. All impedance measurements were recorded between 10 mHz and 5.0 kHz with an ac amplitude of 10 mV.

RESULTS AND DISCUSSION

Electrochemical polymerization

Figures 2(a) and 2(b) show the comparison of a silent and a sono-voltammograms of 3MT, respectively. The electrolytic medium is composed of 0.05*M* 3MT, 0.1*M* TBATFB/AcN, and the ultrasound (40 W cm^{-2}) was applied with a face-on geometry to the working electrode. The hydrodynamic nature of the sono-voltammogram is clear as shown in Figure 2(b). However, in contrary to sono-electrochemical redox processes taking place in the bulk such as in the case of $Ru(NH_3)_6^{2+}/Ru(NH_3)_6^{+3}$ in 0.1*M* KCl,[20] the shape of the insonated cyclic voltammogram did not exhibit the same expected behavior of a silent voltammogram at a microelectrode. A limiting-current is reached, which is characterized by the appearance of current oscillations for the later electrode. A statistical treatment of the current data between +1.35 V and +1.70 V shows that a plateau is reached. A unique difference in this case is that oxidation of 3MT results in the formation of a conducting polymeric layer that deposits on the platinum substrate. During the forward scan of the sono-voltammogram, and when the potential reaches a value of ca. +0.8 V, the current starts to increase appreciably, indicating the onset of the polymer film formation. The current reaches quasi steady state characteristics with the appearance of two semidiscrete peaks (that eventually averages to a limiting current plateau-like) and are relatively higher than that obtained in the silent votammetric experiment. The fluctuations observed in Figure 2(b) are superimposed on the faradaic component of the current that results in the film formation. This current ''noise'' is consistent with the turbulent nature of the macroscopic jet of liquid and with the presence of oscillating and cavitations bubbles.[21] As the reverse cycle (reduction) of the voltammogram starts, the reduction of the polymer film that formed during the forward cycle starts. The magnitude of the quasi-limiting current of the sono-voltammogram depends on the distance separating the horn from the surface of the electrode and on the ultrasound intensity as shown in Figures 3(a) and 3(b), respectively. The observed effects depicted in Figure 3 are consistent with those published earlier for other sono-electrochemical experiments.[22] The relation between different experimental conditions and limiting current, I_{lim}, are given from the following relation for semi-infinite spherical diffusion:[23]

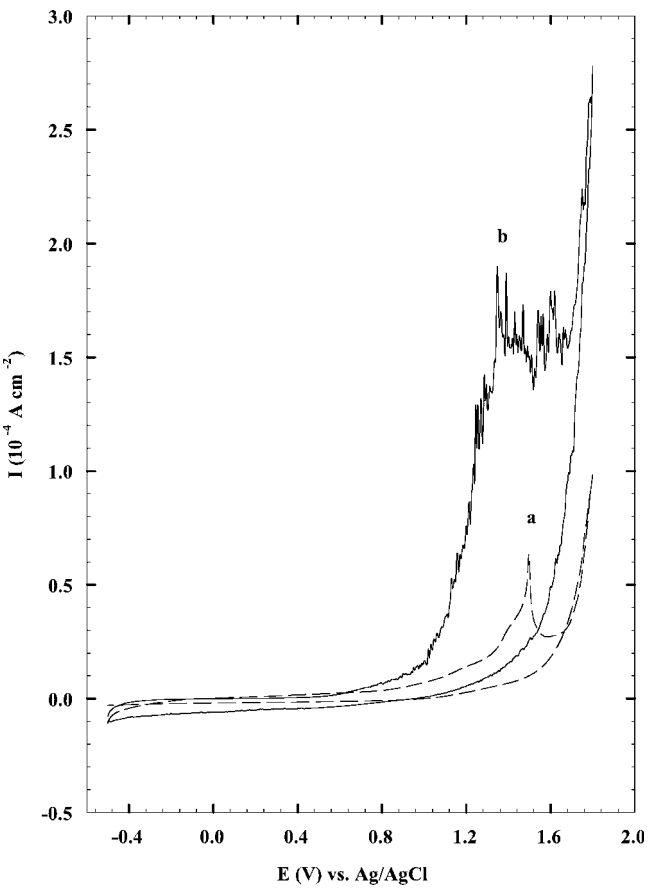

Figure 2 Comparison of silent voltammogram (a) and sono-voltammogram (b) for the oxidation of 0.05*M* 3MT in 0.1*M* TBATFB/AcN on a platinum electrode disc electrode (radius 6 mm) using 3 mm horn-tip and 40 mm electrode-to-horn distance (40 W cm^{-2}), scan rate 50 mV s^{-1}.

$$I_{\text{lim}} = \frac{nFADC}{\delta} \tag{1}$$

n is the number of transferred electrons, F is Faraday constant, D is the diffusion coefficient, A is the electrode area, C is the concentration, and δ is the thickness of diffusion layer. The large anions, causing the doping of the polymer, in the solution are attracted to the opposite potential at the surface of the electrode. When the accumulation of the charges is hindered by their diffusion through the film, they start to be swept by the stream caused by the sonication. The change in sono-source intensity and the variation of its distance to the electrode surface will affect the diffusion layer thickness and its shape, and therefore, should affect the electrochemical polymerization of 3MT. Thus, the morphology, doping level, and conductivity of the resulting polymer films varied with the later effects. Table I shows the elemental microanalysis of PMT films grown under different conditions in LPC/AcN. The results prove that the films are composed of polymerized 3MT. The doping level as well as the conductivity of the resulting films increases as the distance separating the horn and the electrode decreases. The noticeable increase in the conductivities of the films with the level of doping was reported earlier.[24] In the case of using a sono-source during the electro-polymerization step, the increase in the micro-agitation that develops through the diffuse layer and the enhancement of the diffusion of the monomer and electrolytic species should result in more homogeneous films. On the other

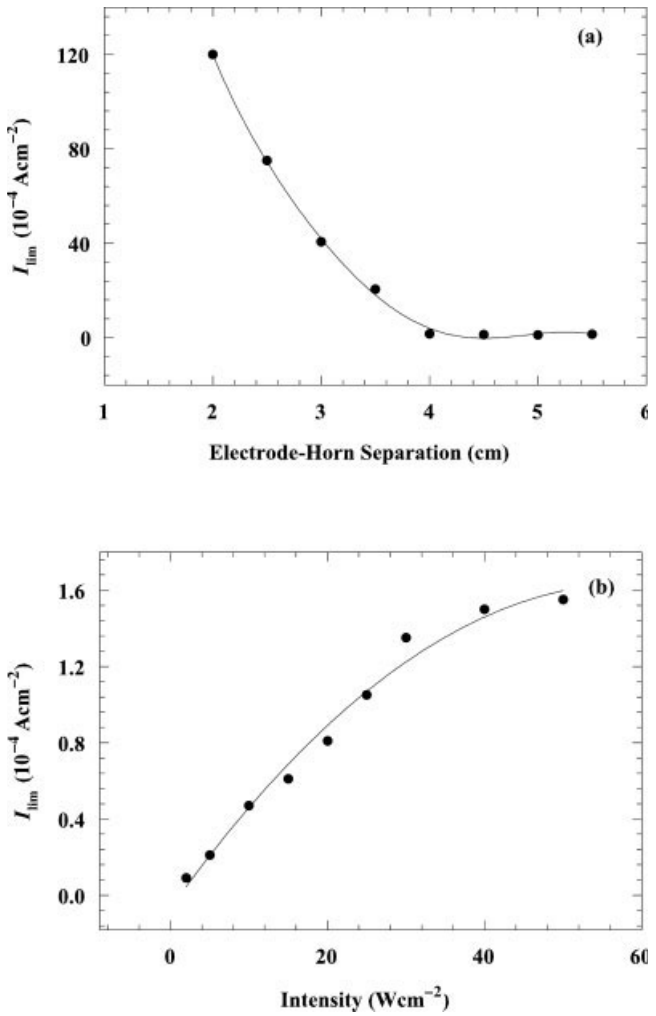

Figure 3 (a) Relation between the limiting current, I_{lim}, recorded from the sono-voltammogram of 0.05*M* 3MT in 0.1 TBATFB/AcN at 0.03 cm^2 Pt disc electrode, and various horn-to-electrode distances (40 W cm^{-2}, 20 kHz, 50 mV s^{-1}). (b) Relation between the limiting current, I_{lim}, recorded from the sono-voltammogram of 0.05*M* 3MT in 0.1 TBATFB/AcN, and various ultrasonic intensities (0.03 cm^2 Pt disc electrode, 20 kHz, 50 mV s^{-1}).

hand, the level of doping was affected by the morphology of the resulting film and the rate of diffusion of the corresponding anions into the film. Moreover, the four-probe measurements determined the ''surface'' conductivity of the film rather than its bulk. Thus, films prepared under silent conditions show relatively higher surface conductivity and relative surface-rich doped films with decreased horn to electrode distance. The SEM results proved the above explanation in terms of the contribution of the morphology to the resulting conductivity of the film as will be discussed later. Further decrease in the distance of the horn resulted in the damage of the formed polymer film.[25]

Infrared and X-ray photoelectron spectroscopies

FTIR spectrum of a KBr pressed pellet of PMT grown under constant applied potential of 1.70 V and ultrasonic irradiation of 40 W cm^{-2} is shown in Figure 4. The numbers of scans collected at a resolution of 2 cm^{-1} and with an accuracy of 0.004 cm^{-1} were 64. The assignments of the principal absorption bands are the following: the bands between 860 and 460 cm^{-1} are due to the C—H out-of-plane vibrations, the absorption band at 856 cm^{-1} is attributed to the ring C—H out-of-plane bending vibration, that is specific for the 2,5-disubstituted thiophene rings, and the absorption peak at 1630 cm^{-1} is due to the deformation vibration of the methyl group. The ill-defined band at 1300 cm^{-1} and that at 1460 cm^{-1} are attributed to the stretching vibration of the 2,3,5-trisubstituted thiophene rings. Two small absorption bands appeared at 2850 and 2922 cm^{-1}, respectively, are attributed to the deformation vibrations of the methyl group. The above data confirms that the application of the sono-radiation source did not affect the structural regularity of the repeat units in the chain, the α-α′-couplings between the 3MT units are predominant, and the aromatic ring integrity was maintained in the film.

X-ray photoelectron spectroscopy (XPS) measurements were performed on PMT films grown at +1.70 V (versus Ag/AgCl) and ultrasonic irradiation of 40 W cm^{-2}. Figure 5 shows the XPS spectra of PMT film formed potentiostatically at +1.70 V under ultrasonic irradiation (40 W cm^{-2}, 20 kHz, 4.0 cm electrode-to-horn separation). The data of the atomic concentration

TABLE I
Elemental Microanalysis, Empirical Formula, and Conductivities of Poly(3-methylthiophene) Films

Sample	Elemental microanalysis C (%)	H (%)	S (%)	Cl (%)	Empirical formula	Conductivity (10 S cm^{-1})
Film (1)[a]	53.4	3.91	28.5	6.91	$C_{5.00}H_{4.40}S_{1.00}Cl_{0.22}$	9.20
Film (2)[b]	60.1	3.97	29.6	4.30	$C_{5.00}H_{3.96}S_{0.92}Cl_{0.12}$	0.0135
Film (3)[b]	58.3	3.98	30.1	5.80	$C_{5.00}H_{4.10}S_{0.97}Cl_{0.17}$	0.168
Film (4)[b]	55.6	3.96	29.3	6.67	$C_{5.00}H_{4.20}S_{0.99}Cl_{0.21}$	1.81

[a] Film prepared under silent potentiostatic condition, E_{appl} = +1.75 V.
[b] Films prepared under sono-electrochemical conditions, E_{appl}= +1.75 V, 40 W cm^{-2}, 20 KHz, 50 mm, 40 mm, and 30 mm electrode-to-horn distances, respectively.

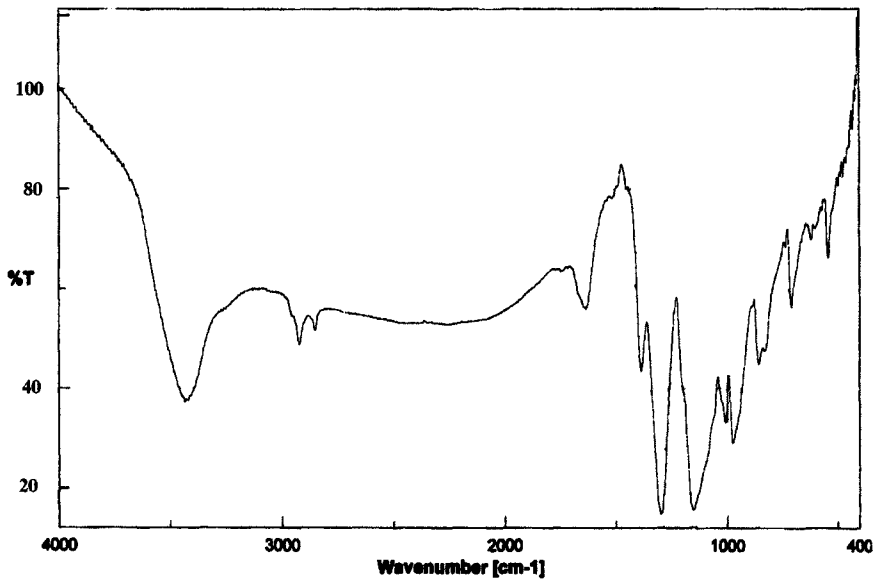

Figure 4 FTIR spectrum of KBr pressed-pellet of as-grown PMT film formed potentiostatically ($E_{ap} = 1.75$ V versus Ag/AgCl, 40 W cm^{-2}, 20 kHz).

of elements as calculated from the XPS experiments are given in Table II. The data are shown for films analyzed at the film/electrolyte (0.1*M* TBATFB/AcN) interface. As could be noticed from the data in Table II, the F/B atomic ratios (4.3, 2.5, 2.7, 3.8) show deviation from the ideal F/B stoichiometric ratio of 4 for the oxidized films at +1.2 V.[26] The films formed under sono-electrochemical irradiation conditions and with variable electrode-to-horn separation distances (30–50 mm), on the other hand, showed an appreciable fluorine deficiency and a decrease in the F/B ratio with distance. Furthermore, the results of Table II revealed an important fact; the coexistence of both cation and anion in the film is likely, which is similar to the neutral ''undoped'' state of the film. This fact is noticed from the constant B/N atomic concentration ratio, which was calculated from XPS-1S peaks for films obtained and analyzed under different experimental conditions. These ratio values were 0.90, 1.0, 1.1, and 0.99 for the samples analyzed, respectively. In the case of films formed under sono-electrochemical irradiation conditions, the closer the electrode-to-horn distance the higher is the ion content. It is also important to notice that there is an ion-pairing effect rather than a single cation effect on film behavior during the doping process that takes place for films formed under sono-electrochemical conditions.

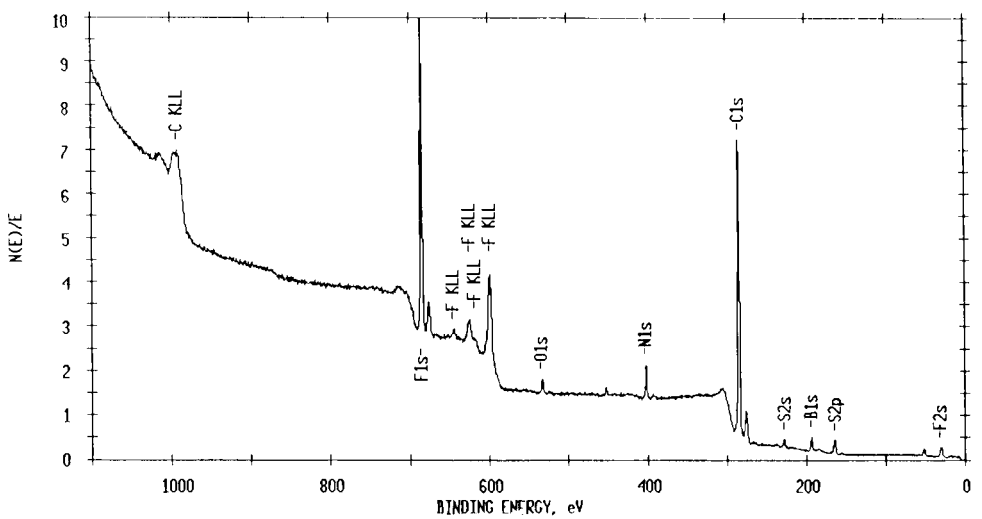

Figure 5 XPS spectra of PMT film formed potentiostatically at +1.75 V under ultrasonic irradiation (40 W cm^{-2}, 20 kHz, 40 mm electrode-to-horn separation).

TABLE II
Atomic Concentration of Elements from XPS Measurements for Films Synthesized under Silent Potentiostatic Conditions,[a] and under Sono-Electrochemical Conditions[b]

	Atomic concentration (%, w/w)			
Element	Film 1	Film 2	Film 3	Film 4
C1	57.4	63.64	63.06	62.19
O1	3.68	9.23	8.08	3.80
S1	4.76	6.56	6.91	5.75
F1	22.8	11.6	12.7	18.5
B1	5.41	4.57	4.79	4.85
N1	5.98	4.37	4.46	4.91

[a] $E_{appl} = +1.75$ V (Film 1).
[b] $E_{appl} = +1.75$ V, 40 W cm^{-2}, 20 KHz, 50 mm, 40 mm, and 30 mm electrode-to-horn distances, for film 1, film 2, and film 3.

Scanning electron microscopy

The effect of using ultrasonic irradiation during the electrochemical synthesis of PMT resulted in different morphological structures of the solution-side resulting film. Five-member heterocycles such as thiophenes, pyrroles, furans, and selenophenes electropolymerize through an α-α′ coupling. This results in a highly ordered chain provided that the coplanarity of the units within the chains is also respected. This later property could be controlled by restricting the electrochemical synthesis conditions and more importantly by planning the number and extent of substitution in the β-position of the monomeric starting compounds. This is due to the fact that among the structural defects that can change the ''regularity'' of the configuration are the unlikely α-β′-couplings. However, the chain packing density that can affect the compactness/porosity and homogeneity of the film should be a function of the diffusion of the oxidized monomeric/doping species to the electrode surface as well as other factors such as hydrophobic character of the film. Thus, the application of the ultrasonic irradiation with controlled power, duration, and electrode-to-horn distance will result in films with distinct morphologies. Thick films (ca. $>$ 3000 Å, as estimated from the charge passing during the polymerization) grown on platinum substrates appeared fully amorphous and have swollen lumps (mainly due to electrolyte presence) as shown in Figure 6(a). SEM pictures for films prepared under sono-electrochemical conditions (40 W cm^{-2} and 20 kHz) for different electrode-to-horn separations are given in Figures 6(b), and 6(c), respectively. The surfaces of the sono-electrochemically synthesized films are more compact than those formed using silent electrochemical condition. However, the grain size of the polymer film increases as the distance between the electrode and the horn decreases. Polymer chains rearrangement is expected to take place and cavitations effect is also noticed. Structural defects and reticulation were observed when the horn approaches the electrode surface with a distance less than 3.0 cm. The electrochemical activity of the films was examined by cycling the polymer between two potential limits (ca. −0.2 V to +1.2 V) repeatedly (data not shown) in a monomer-free electrolyte (0.05*M* TBATFB/AcN). The films prepared under sono-electrochemical conditions showed no appreciable decrease in the current measured from the I/E curves ($\sim$ 1.2% loss in activity).

Electrochemical impedance spectroscopy

Equivalent electrical circuits were used to interpret results from EIS data.[27,28] The equivalent circuit used in this study is illustrated in Figure 7(a). The components of the circuits are (i) resistor, R_s, which simulates the resistive behavior of the electrode and electrolyte, (ii) constant phase elements, CPE, defined as follows:

$$Z_{CPE} = A_{CPE}(j\omega)^{-\alpha}_{CPE} \quad (2)$$

where A is a frequency independent constant, ω is the angular frequency, and α_{CPE} is a dimensional factor, and (iii) a diffusion element, Z_W, that describes the diffusion of ions through the polymer film.[29] As can be noticed in Figures 7(b) and 7(c), the shape of the impedance diagram for PMT differs significantly as the applied potential to the electrode is stepped from the relatively ''undoped'' (ca. $E_{appl} = 0$ V) to the oxidized or ''doped'' (ca. $E_{appl} = +1.5$ V). The Bode plot for polymer films subjected to potential values of 0 V has a phase minima at intermediate frequencies. The onset of an impedance plateau and the phase maximum at the low frequency region for films prepared under silent electrochemical conditions indicates the contribution of a diffusion process.[30] The films prepared under sono-electrochemical conditions, on the other hand, displayed similar impedance behavior with less contribution of the diffusion at the same frequency ranges. A similar trend for the impedance plateau was also observed when the applied potentials shifted in the anodic direction for both films. Moreover, when the applied potential to the electrode reaches +1.5 V, the impedance plateau for the film extends to the intermediate frequency ranges. The results show that the impedance value decreases with the applied potential for both films up to +1.0 V that is followed by an increase when the applied potential reaches a value of +1.5 V. This is due to the fact that the level of doping in both types of films increases with potential, and as the applied potential reaches +1.5 V, the physical integrity of the polymer layer is not retained and resulted in the relative loss of its electrical conduction. However, the films prepared under sono-electrochemical conditions have relatively higher impedance values compared to those prepared under silent condi-

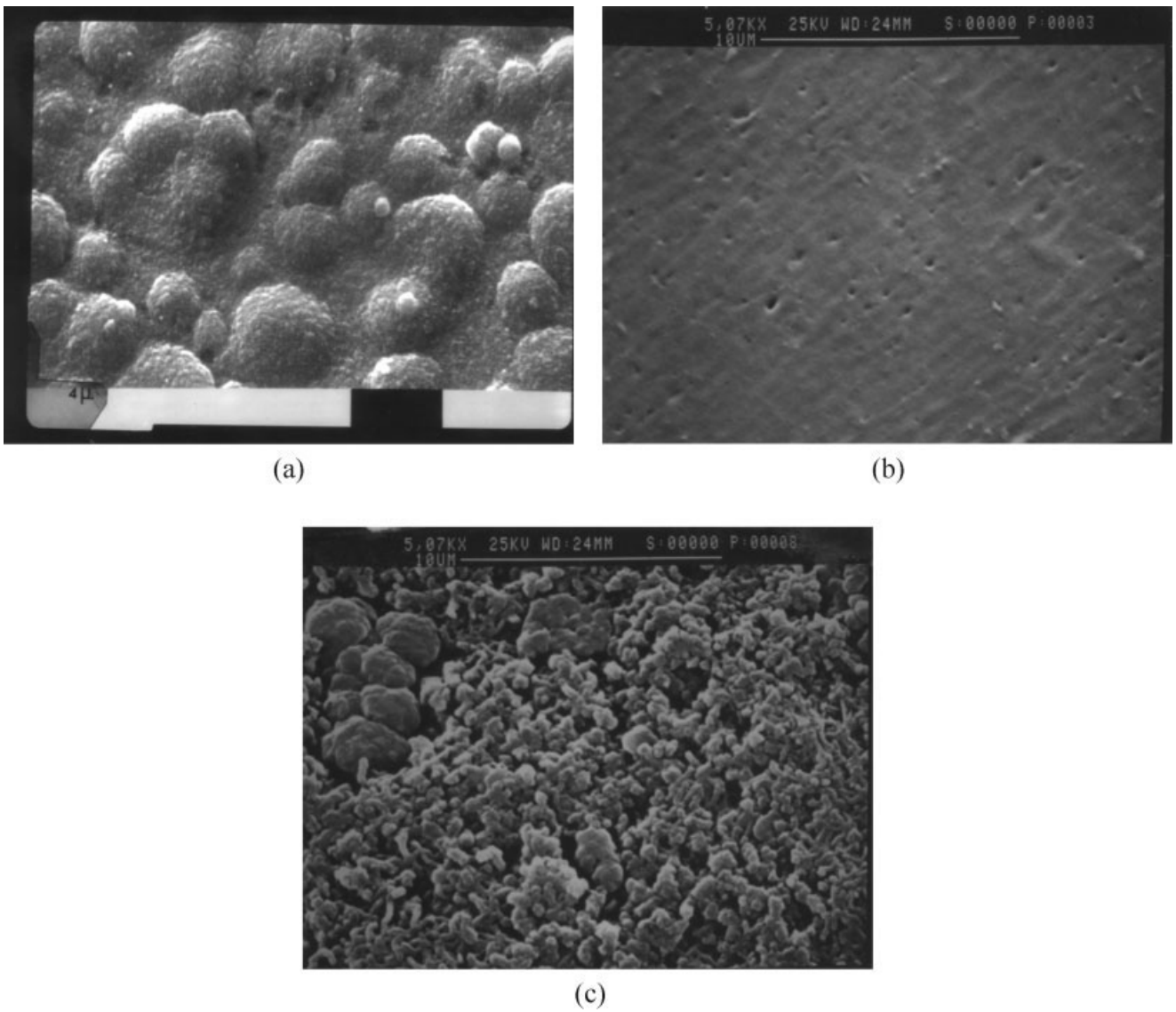

Figure 6 (a) SEM pictures of PMT films prepared under silent potentiostatic conditions for 30 s ($E_{appl} = +1.5$ V) from 0.05 3MT, 0.1*M* TBATFB/AcN. (b) SEM pictures of PMT films prepared under sono-electrochemical potentiostatic conditions for 30 s ($E_{appl} = +1.75$ V), 40 W cm^{-2}, 20 KHz, 40 mm electrode-to-horn distance. (c) SEM pictures of PMT films prepared under sono-electrochemical potentiostatic conditions for 30 s ($E_{appl} = +1.75$ V), 40 W cm^{-2}, 20 KHz, 30 mm electrode-to-horn distance.

tions. These data are in good agreement with the CV and elemental analysis results. Table III represents the values calculated for R_s, R_{ct}, CPE, α_{CPE1}, and Z_W in the simulation of the impedance experiments. The R_s value is related to the electrolyte resistance and some contribution of high frequency resistive components of the polymer electrode processes. For both films, prepared under silent and sono-electrochemical conditions, the R_s value is high in the reduced (undopped) state at E_{appl} of $\sim$ 0 V. The value decreases as the applied potential increases in the positive (doping) direction and the film prepared under silent conditions has less R_s values. Again, the increase in the R_s value as $E_{appl} = +1.5$ V is indicative of the loss of the electrical conductivity of the film. The R_{ct} is considered here as the charge transfer resistance associated with the interface polymer/electrolyte and is inversely related to the charge transfer kinetic facility at the electrode/electrolyte interface. Again, with the relatively low electronic conduction through the films (at low E_{appl}), the value of R_{ct} decreases with the applied potential. The films prepared under sono-electrochemical conditions display relatively higher R_{ct} values. The later is explained in terms of the relatively lower doping level, which is in good agreement with the elemental analysis and XPS data. Moreover, the R_{ct} value showing the highest value when $E_{appl} = +1.5$ V for both films. The CPE is the constant phase element and equal to the double layer capacitance (C_{dl}) produced by charge accumulation at the polymer/electrolyte

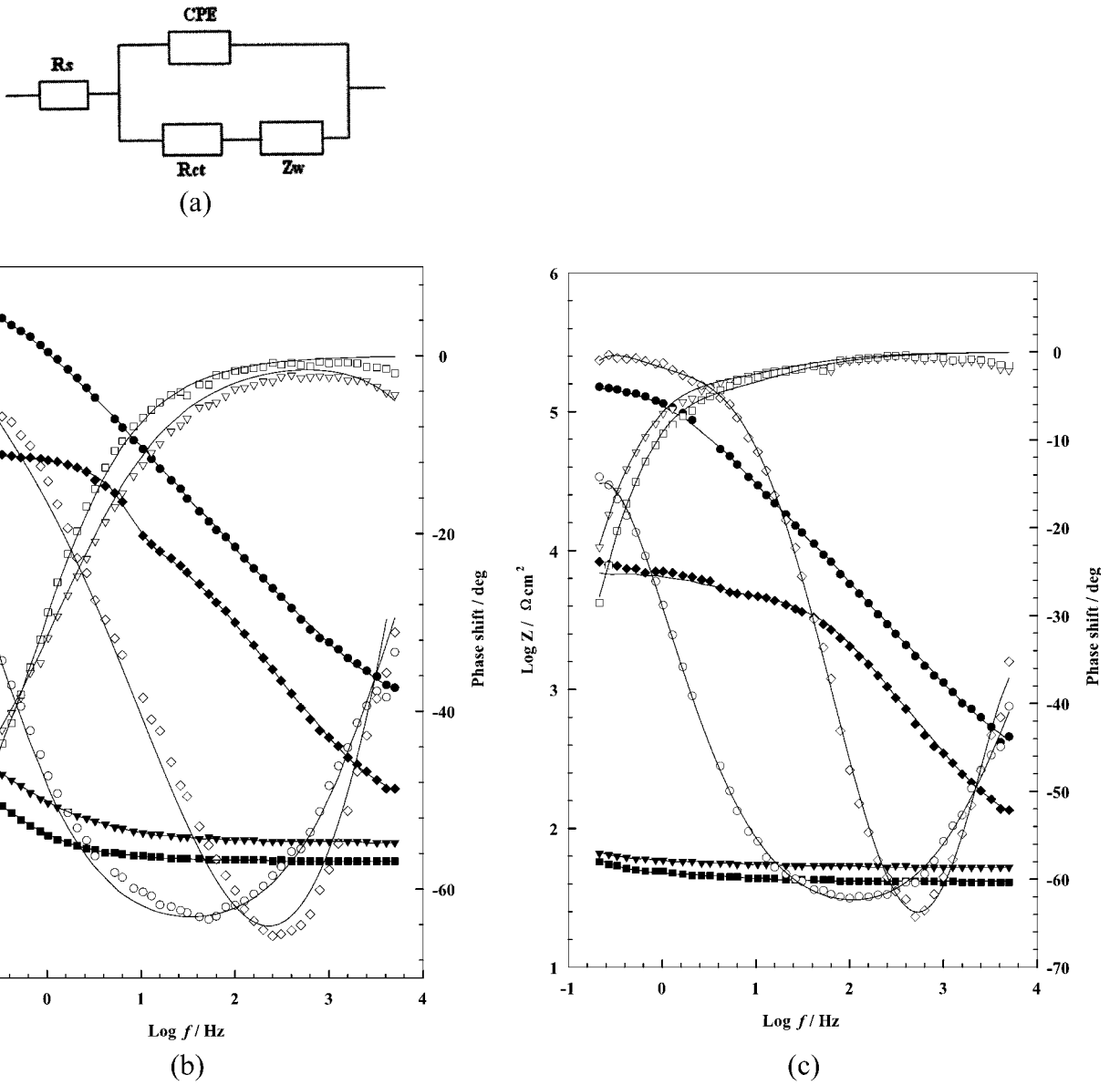

Figure 7 (a) Equivalent circuit used in the fit procedure of the impedance spectra of Figures 7(a)–7(c). The results were analyzed using Levenberg-Marquardt/Simplex algorithms based on a complex nonlinear least-squares procedure. (b) Bode plots of PMT films prepared (from 0.05 3MT, 0.1*M* TBATFB/AcN) under silent potentiostatic conditions for 30 s ($E_{appl} = +1.5$ V) in 0.1*M* TBATFB, data are shown for different dc voltages of 0.0 V (■), +0.7 V (▼), +1.0 V (◆), and + 1.5 V (●), respectively. Solid lines represent simulated data based on the parameters of equivalent circuit of Figure 7(a) (Solid symbols for Modulus/frequency, and white symbols for Phase shift/frequency). (c) Bode plots of PMT films prepared (from 0.05 3MT, 0.1*M* TBATFB/AcN) under sono-electrochemical potentiostatic conditions for 30 s ($E_{appl} = +1.75$ V), 40 W cm^{-2}, 20 KHz, 40 mm electrode-to-horn distance in 0.1*M* TBATFB, data are shown for different dc voltages of 0.0 V (■), +0.7 V (▼), +1.0 V (◆), and + 1.5 V (●), respectively. Solid lines represent simulated data based on the parameters of equivalent circuit of Figure 7(a) (Solid symbols for Modulus /frequency, and white symbols for Phase shift/frequency).

interface. The values of CPE displayed in Table III are relatively larger than those expected for the double layer capacitance, C_{dl}. Also, the values calculated for the empirical parameter α_{CPE} are not equal to 1 because of the expected roughness of the films compared to the ideal flat working electrode surface. It was experimentally established that the admittance, Y, represents the double-layer charging and depends on the frequency. The frequency dispersion of CPE in the impedance representation is given by[31]

$$Z_{CPE} = Y_{CPE}^{-1} = Y_0^{-1}(j\omega)^{-\alpha} \tag{3}$$

where $j = \sqrt{-1}$, and ω is the radial frequency. Again, CPE values are highest at the two ''extreme'' voltages with gradual decrease as the applied potential increases

TABLE III
Parameters Corresponding to the Equivalent Circuit in Figure 7(a) and Obtained from the Simulation of the Impedance Curves for the Films Prepared under Silent Potentiostatic Conditions

$R_s/\Omega\ cm^2$	$R_{ct}/\Omega\ cm^2$	$Y_o/\mu F\ cm^{-2}\ s^{\alpha}$	α	$Z_W/k\Omega\ cm^{-2}\ s^{1/2}$	E_{app}/V
Silent potentiostatic conditions[a]					
227	1.68×10^5	7.71×10^5	0.761	–[b]	0.0
53.4	68.5	36.5	0.722	0.955	+0.7
41.9	64.9	33.7	0.712	0.874	+1.0
86.5	5.48×10^3	5.69×10^5	0.852	1.65	+1.5
±0.4[c]	±0.7[c]	±1.2[c]	±0.003[c]	±0.017[c]	–
Sono-electrochemical potentiostatic conditions[d]					
701	7.44×10^5	1.19×10^6	0.737	–[b]	0
89.8	289	385	0.652	1.16	0.7
66.4	224	214	0.732	3.50	1
159	1.32×10^4	9.01×10^5	0.873	3.62	1.5
±0.3[c]	±0.6[c]	±0.9[c]	±0.003[c]	±0.05[c]	–

[a] For 30 s ($E_{appl} = +1.75$ V).
[b] Negligible contribution.
[c] Mean error values.
[d] For 30 s ($E_{appl} = +1.75$ V), 40 W cm^{-2}, 20 KHz, and 40 mm electrode-to-horn distance.

for both films. The Warburg impedance representing the ''infinite'' diffusion of the electroactive species is given by:[31]

$$Z_W = \sigma(\omega)^{1/2}(1 - j) \tag{4}$$

where σ is the Warburg coefficient and is defined as

$$\sigma = \frac{RT}{n^2F^2A\sqrt{2}}\left(\frac{1}{C_O^*\sqrt{D_O}} + \frac{1}{C_R^*\sqrt{D_R}}\right) \tag{5}$$

where D_O and D_R are the diffusion coefficients for oxidants and reductants, respectively. This form of the impedance is only valid if the diffusion layer has an infinite thickness. In the case of the polymer film, the diffusion layer is bounded and the impedance at lower frequencies no longer obeys eq. (4), instead the following expression is used:

$$Z_O = \sigma\omega^{1/2}(1 - j)\ \tanh\left[\delta\left(\frac{j\omega}{D}\right)^{1/2}\right] \tag{6}$$

and δ is the Nernst diffusion layer thickness. A noticeable increase in the Warburg coefficient is observed with E_{appl} as indicated in Table III. The films prepared under sono-electrochemical conditions have relatively higher values. Thus, considerable difference in this parameter was observed when comparing the two films prepared under different conditions. This is attributed to the clear difference in the morphology and porosity of the films and is in good agreement with the SEM pictures.

CONCLUSIONS

Polymer films prepared under sono-electrochemical conditions have distinct morphologies due to the influence of the irradiation on the diffuse layer during the synthesis step. The level of doping of the resulting polymer films varies with the electrode-to-horn distance during the synthesis. The shorter the distance the higher the level of doping and consequently the surface conductivity of the film increases. The compactness of the film and less porous structures resulted in less ionic diffusion within the films. EIS data showed that the restriction of diffusion and less level of doping affected the rate of charge transfer at the polymer/electrolyte interface and the diffusion parameters of the film. The diffuse layer develops with the oxidized sites and counter-ions at the polymer/electrolyte interface. As the polymer is subjected to higher positive applied potentials, a transition is seen in the impedance spectra indicating the onset of doping. Diffusion is more pronounced with films prepared under silent conditions and when the polymer film is over-oxidized at an applied potential of ca. +1.5 V. FTIR spectra of the film and elemental analyses showed that the integrity of the films were maintained with α-α'-couplings between the 3MT predominantly throughout the chain.

The author is indebted to the University of Cairo (office of Vice-president for Research) through the ''Young Investigator Program,'' and to the US-NSF program for the partial financial support. Special thanks to the Department of Chemistry of the University of Cincinnati for allowing the use of the four-probe and XPS facilities.

References

1. Apetrei, C.; Rodriguez-Mendez, M. L.; Parra, V.; Gutierrez, F.; de Saja, J. A. Sens Actuators B 2004, 103, 145.
2. Vecino, M.; Gonzalez, I.; Munoz, M. E.; Santamaria, A.; Ochoteco, E.; Pomposo, J. A. Polym Adv Technol 2004, 15, 560.
3. Moliton, A.; Hiorns, R. C. Polym Int 2004, 53, 1397.

4. Hamer, W. J.; Koene, L.; de Wit, J. H. W. Mater Corros 2004, 55, 653.
5. Sarma, T. K.; Chattopadhyay, A. J Phys Chem A 2004, 108, 7837.
6. Zhou, J.; Fisher, E. R. J Nanosci Nanotechnol 2004, 4, 539.
7. Onoda, M.; Kato, Y.; Shonaka, H.; Tada, K. Electr Eng Jpn 2004, 149, 7.
8. Tamirisa, P. A.; Liddell, K. C.; Pedrow, P. D.; Osman, M. A. J Appl Polym Sci 2004, 93, 1317.
9. Barton, A. C.; Collyer, S. D.; Davis, F.; Gornall, D. D.; Law, K. A.; Lawrence, E. C. D.; Mills, D. W.; Myler, S.; Pritchard, J. A.; Thompson, M.; Higson, S. P. J. Biosens Bioelectron 2004, 20, 328.
10. Takagi, K.; Mori, K.; Kunisada, H.; Yuki, Y. Polym Bull 2004, 52, 125.
11. Wang, J. Z.; Hu, Y.; Song, L.; Chen, Z. Y. Solid State Ionics 2004, 167, 425.
12. Chowdhury, A. N.; Atobe, M.; Nonaka, T. Ultrason Sonochem 2004, 11, 77.
13. Lindermeir, A.; Horst, C.; Hoffmann, U. Ultrason Sonochem 2003, 10, 223.
14. Banks, C. E.; Compton, R. G. Electroanalysis 2003, 15, 329.
15. Eklund, J. C.; Marken, F.; Rebbitt, T. O.; Akkermans, R. P.; Waller, D. N. Electrochim Acta 1997, 42, 2919.
16. Osawa, S.; Ito, M.; Tanaka, K.; Kuwan, J. Synth Met 1987, 18, 145.
17. Akbulut, U.; Toppare, L.; Yurttas, B. Polymer 1986, 27, 803.
18. Holtzknecht, L. J.; Mark, H. B., Jr.; Ridgway, T. H.; Zimmer, H. Anal Instrum 1989, 18, 23.
19. Barsoukov, E.; Macdonald, J. R., Eds. Impedance Spectroscopy, Theory, Experiment, and Applications, 2nd ed.; Wiley-Interscience: New York, 2005.
20. Banks, C. E.; Rees, N. V.; Compton, R. G. J Electroanal Chem 2002, 535, 41.
21. Klima, J.; Bernard, C.; Degrand, C. J Electroanal Chem 1994, 367, 297.
22. Compton, R. G.; Eklund, J. C.; Page, S. D.; Mason, T. J.; Walton, D. J. J Appl Electrochem 1996, 26, 1775.
23. Brett, C. M. A.; Brett, A. M. O. Electrochemistry: Principles, Methods, and Applications; Oxford University Press: Oxford, 1994; 155 pp.
24. Hotta, S.; Simotsuma, W. Synth Met 1985, 11, 139.
25. Cassaie, E.; Porter, R. S. Polymer Stress Reaction, Vol. 2; Academic Press: New York, 1979.
26. Yamamoto, T.; Sanechika, K.; Yamamoto, A. J Polym Sci Part C: Polym Lett 1980, 18, 9.
27. Gazotti, W. A.; Matencio, T.; Marco- A. P. Electrochim Acta 1998, 43, 457.
28. Köleli, F.; Röpke, T.; Hamann, C. H. Electrochim Acta 2003, 48, 1595.
29. Albery, W. J.; Mount, A. R. J Electroanal Chem 1991, 305, 3.
30. Perloni, P.; Mastragostino, M.; Meneghello, L. Electrochim Acta 1996, 41, 27.
31. Sluyters-Rehbach, M. Pure Appl Chem 1994, 66, 1831.